

Electronic Supporting Information (ESI)

Aqueous Solutions of Binary Ionic Liquids: Insight into Structure, Dynamics, and Interface Properties by Molecular Dynamics Simulations

Maryam Heydari Dokoochaki^a, Amin Reza Zolghadr^{*a}, Mohammad Hadi Ghatee^{*a}, Axel Klein^{*a,b}

^a Department of Chemistry, Shiraz University, Shiraz, 71946-84795, Iran

^b Department für Chemie, Institut für Anorganische Chemie, Universität zu Köln, Greinstraße 6, D-50939 Köln, Germany

*E-mail: arzolghadr@shirazu.ac.ir; Tel: +98 71 3613 7157; ORCID: 0000-0002-6289-3794

*E-mail: mhghatee@shirazu.ac.ir; ORCID 0000-0001-6567-9091

*E-mail: axel.klein@uni-koeln.de; Tel.: +49-221-470-4006; ORCID: 0000-0003-0093-9619

Contents

Supporting Tables:

Table S1. Calculated radial distribution functions (RDF) – distances (\AA) and relative intensities (in parentheses) of the first peaks.

Table S2. Diffusion coefficients (D_i) ($10^{-6} \text{ cm}^2 \text{ s}^{-1}$) calculated from the MSD-time curves in NPT ensemble.

Table S3. Diffusion coefficients (D_i) ($10^{-6} \text{ cm}^2 \text{ s}^{-1}$) calculated from the MSD-time curves of $[\text{C}_4\text{mim}][\text{BF}_4]/[\text{PF}_6]$ /water system with different pressure coupling constants.

Table S4. DFT calculated H-bond distances ($\text{H}_2\cdots\text{X}$ and $\text{HW}\cdots\text{X}$, ($\text{X} = \text{Cl}, \text{F1 or F2}, \text{OW}$)) with angles ($\text{C}_2\text{-H}_2\text{-X}$ and $\text{OW}\text{-HW-X}$) shown in parenthesis for different complexes.

Table S5. Number of hydrogen-bonds between ILs and water molecules per time frame.

Supporting Figures:

Figure S1. Figure S1. Radial distribution functions for the $\text{H}_2\cdots\text{OW}$ interactions (A) $[\text{C}_4\text{mim}][\text{Cl}]/[\text{BF}_4]$ /water, (B) $[\text{C}_4\text{mim}][\text{Cl}]/[\text{PF}_6]$ /water, (C) $[\text{C}_4\text{mim}][\text{BF}_4]/[\text{PF}_6]$ /water mixtures.

Figure S2. Radial distribution functions for $\text{C}_6\cdots\text{X}$ and $\text{C}_{10}\cdots\text{X}$ interactions ($\text{X} = \text{Cl}, \text{F1 or F2}$) (A) $[\text{C}_4\text{mim}][\text{Cl}]/[\text{BF}_4]$ /water, (B) $[\text{C}_4\text{mim}][\text{Cl}]/[\text{PF}_6]$ /water, (C) $[\text{C}_4\text{mim}][\text{BF}_4]/[\text{PF}_6]$ /water mixtures.

Figure S3. Radial distribution functions for the $\text{OW}\cdots\text{HW}$ interactions in all aqueous mixtures.

Figure S4. Combined radial/angular distribution functions of anion-water for $[\text{C}_4\text{mim}][\text{Cl}]/[\text{PF}_6]$ /water and $[\text{C}_4\text{mim}][\text{BF}_4]/[\text{PF}_6]$ /water systems.

Figure S5. Combined radial/angular distribution functions of cation-anion for $[\text{C}_4\text{mim}][\text{Cl}]/[\text{PF}_6]$ /water and $[\text{C}_4\text{mim}][\text{BF}_4]/[\text{PF}_6]$ /water systems.

Figure S6. Combined radial/angular distribution functions for water-anion interactions of (A) $[\text{C}_4\text{mim}][\text{Cl}]/[\text{BF}_4]$ /water, (B) $[\text{C}_4\text{mim}][\text{Cl}]/[\text{PF}_6]$ /water, and (C) $[\text{C}_4\text{mim}][\text{BF}_4]/[\text{PF}_6]$ /water systems.

Figure S7. Mean-square displacements (MSDs) over 10 ns of simulation of the (A, B) $[\text{C}_4\text{mim}][\text{Cl}]/[\text{BF}_4]$, (C, D) $[\text{C}_4\text{mim}][\text{Cl}]/[\text{PF}_6]$, and (E, F) $[\text{C}_4\text{mim}][\text{BF}_4]/[\text{PF}_6]$ systems. Left panel (A, C, and E) for the water-free systems and right panel the aqueous systems (B, D, and F).

Figure S8. Dimer Existence Autocorrelation Functions (DACFs) for the (A, B) $[\text{C}_4\text{mim}][\text{Cl}]/[\text{BF}_4]$, (C, D) $[\text{C}_4\text{mim}][\text{Cl}]/[\text{PF}_6]$, and (E, F) $[\text{C}_4\text{mim}][\text{BF}_4]/[\text{PF}_6]$ systems without (left panel, A, C, and E) and with water (right panel, B, D, and F). The ion pairs are defined based on the distance criteria between Cl or F of the anions and the acidic hydrogen atom of the cations H2.

Figure S9. Atomic density profiles of $[C_4mim][Cl]/[BF_4]$ /water/vacuum, $[C_4mim][Cl]/[PF_6]$ /water/vacuum, and $[C_4mim][BF_4]/[PF_6]$ /water/vacuum systems.

Figure S10. Snapshot of the simulation systems $[C_4mim][Cl]/[BF_4]$ /water/vacuum, $[C_4mim][Cl]/[PF_6]$ /water/vacuum, and $[C_4mim][BF_4]/[PF_6]$ /water/vacuum systems.

Figure S11. Bivariate orientation distribution of the $[C_4mim]^+$ cation paired to the anions for the (A) $[C_4mim][Cl]/[BF_4]$ /water/vacuum and (B) $[C_4mim][Cl]/[PF_6]$ /water/vacuum systems.

Figure S12. (A) Molecular electrostatic potential maps for binary IL complexes.

Figure S13. DFT-calculated compositions of highest occupied molecular orbitals (HOMO) and lowest unoccupied molecular orbitals (LUMO) and their energies.

Supporting Equations and Discussions:

Eq. S1

Eq. S2

Dimer lifetimes of ion pairing of ILs

Supporting Tables

Table S1. Calculated radial distribution functions (RDF) – distances (\AA) and relative intensities (in parentheses) of the first peaks.^a

	$[C_4mim][Cl]/[BF_4]$	$[C_4mim][Cl]/[PF_6]$	$[C_4mim][BF_4]/[PF_6]$	$[C_4mim][Cl]/[BF_4]$ /water	$[C_4mim][Cl]/[PF_6]$ /water	$[C_4mim][BF_4]/[PF_6]$ /water
HW···Cl	-----	-----	-----	2.08 (4.38)	1.95 (3.41)	-----
HW···F1	-----	-----	-----	1.62 (1.34)	-----	1.72 (1.25)
HW···F2	-----	-----	-----	-----	1.70 (0.63)	1.72 (0.71)
H2···Cl	2.15 (22.2)	2.23 (22.8)	-----	2.30 (10)	2.19 (9.73)	-----
H2···F1	1.99 (2.92)	-----	2.02 (5.52)	2.10 (2.11)	-----	2.21 (1.91)
H2···F2	-----	2.08 (1.42)	2.02 (2.42)	-----	2.19 (1.10)	2.21 (1.10)
H2···OW	-----	-----	-----	2.08 (1.31)	2.19 (1.22)	2.22 (1.27)
C6···Cl	3.6 (3.66)	3.56 (4.74)	-----	3.70 (2.74)	3.90 (2.19)	-----
C6···F1	3.36 (1.68)	-----	3.42 (3.25)	3.45 (1.97)	-----	3.45 (1.89)
C6···F2	-----	3.38 (1.48)	3.42 (1.69)	-----	3.41 (1.50)	3.45 (1.65)
C10···Cl	3.94 (1.98)	4 (1.56)	-----	3.93 (1.32)	3.89 (1.12)	-----
C10···F1	3.60 (0.82)	-----	3.57 (0.9)	3.70 (1.60)	-----	3.94 (1.06)
C10···F2	-----	3.7 (1.1)	3.57 (0.71)	-----	3.65 (1.07)	3.69 (0.99)
HW···OW	-----	-----	-----	1.20 (12.75)	1.20 (15.50)	1.20 (15.90)

^a RDFs were determined using the gmx rdf utility from the GROMACS package.

Table S2. Diffusion coefficients (D) ($10^{-10} \text{ m}^2/\text{s}$) calculated from the MSD-time curves in NPT ensemble.

species	$[C_4mim][Cl]/[BF_4]$		$[C_4mim][Cl]/[PF_6]$		$[C_4mim][BF_4]/[PF_6]$	
$[C_4mim]^+$	1.2		0.99		1.7	
anion	$[Cl]^-$	$[BF_4]^-$	$[Cl]^-$	$[PF_6]^-$	$[BF_4]^-$	$[PF_6]^-$
	1.6	1.4	1.1	1.0	2.2	1.6
	$[C_4mim][Cl]/[BF_4]$ /water		$[C_4mim][Cl]/[PF_6]$ /water		$[C_4mim][BF_4]/[PF_6]$ /water	

water	73.4		110.8		116.8	
[C ₄ mim] ⁺	20.2		34.9		33.9	
anion	[Cl] ⁻	[BF ₄] ⁻	[Cl] ⁻	[PF ₆] ⁻	[BF ₄] ⁻	[PF ₆] ⁻
	45.3	37.1	59.7	45.5	54.8	43.8

Table S3. Diffusion coefficients (D) (10^{-10} m²/s) calculated from the MSD -time curves of [C₄mim][BF₄]/[PF₆]/water system with different pressure coupling constants.

species	0.5		1		1.5		2		2.5	
water	116.3		113.5		115.6		116.8		115.7	
[C ₄ mim] ⁺	36.5		32.5		34.3		33.9		37.0	
anion	[BF ₄] ⁻	[PF ₆] ⁻	[BF ₄] ⁻	[PF ₆] ⁻	[BF ₄] ⁻	[PF ₆] ⁻	[BF ₄] ⁻	[PF ₆] ⁻	[BF ₄] ⁻	[PF ₆] ⁻
	53.9	47.4	55.0	47.9	49.3	47.1	54.8	43.8	47.9	41.9

Table S4. DFT calculated H-bond distances (H₂···X and HW···X, (X = Cl, F1 or F2, OW)) with angles (C2-H2-X and OW-HW-X) shown in parenthesis for different complexes.

	[C ₄ mim] ₂ [Cl] [BF ₄]	[C ₄ mim] ₂ [Cl] [PF ₆]	[C ₄ mim] ₂ [BF ₄] [PF ₆]	[C ₄ mim] ₂ [Cl] [BF ₄](H ₂ O)	[C ₄ mim] ₂ [Cl] [PF ₆](H ₂ O)	[C ₄ mim] ₂ [BF ₄] [PF ₆](H ₂ O)
HW...Cl	-----	-----	-----	2.28(167)	2.25(172)	-----
HW...F1	-----	-----	-----	1.87(172)	-----	1.94(164)
HW...F2	-----	-----	-----	-----	1.95(163)	2.04(162)
H2...Cl	2.31(152)	2.25(156)	-----	2.37(155)	2.38(152)	-----
H2...F1	3.10(91)	-----	2.02(158)	3.30(97)	-----	1.95(175)
H2...F2	-----	3.05(93)	2.34(122)	-----	2.96(103)	2.36(118)
H2...OW	-----	-----	-----	2.72(125)	2.74(128)	3.02(72)

Table S5. Number of hydrogen-bonds between ILs and water molecules per time frame.^a

	[C ₄ mim][Cl]/[BF ₄]/water	[C ₄ mim][Cl]/[PF ₆]/water	[C ₄ mim][BF ₄]/[PF ₆]/water
[C ₄ mim][Cl]-water	25	23	----
[C ₄ mim][BF ₄]-water	14	----	11
[C ₄ mim][PF ₆]-water	----	10	9

^a The number of hydrogen-bonds was determined using the gmx hbond utility from the GROMACS package.

Supporting Figures

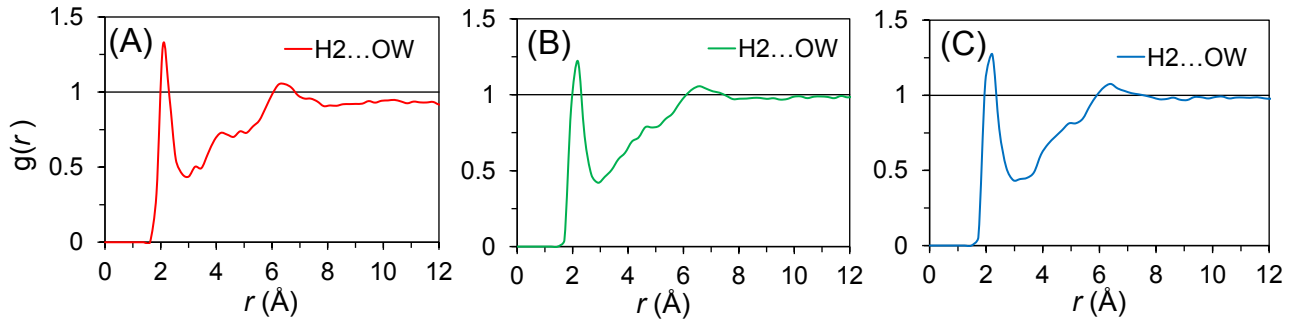


Figure S1. Radial distribution functions for the $\text{H}_2\cdots\text{OW}$ interactions (A) $[\text{C}_4\text{mim}][\text{Cl}]/[\text{BF}_4]$ /water, (B) $[\text{C}_4\text{mim}][\text{Cl}]/[\text{PF}_6]$ /water, (C) $[\text{C}_4\text{mim}][\text{BF}_4]/[\text{PF}_6]$ /water mixtures.

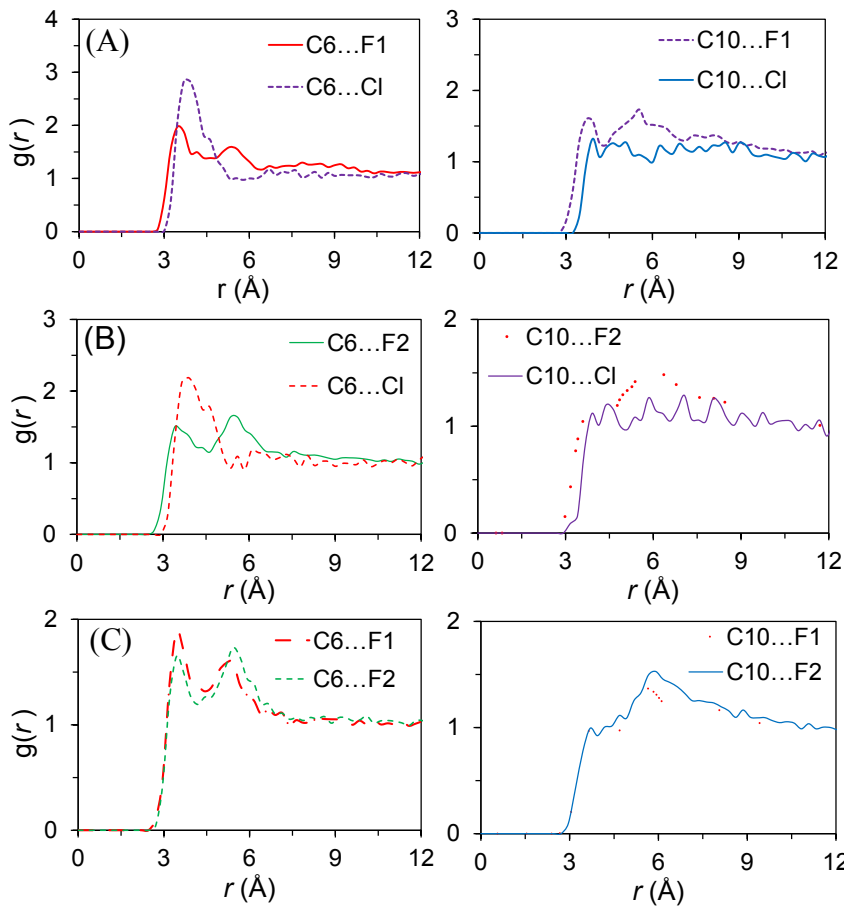


Figure S2. Radial distribution functions for $\text{C}_6\cdots\text{X}$ and $\text{C}_{10}\cdots\text{X}$ interactions ($\text{X} = \text{Cl}, \text{F1}$ or F2) (A) $[\text{C}_4\text{mim}][\text{Cl}]/[\text{BF}_4]$ /water, (B) $[\text{C}_4\text{mim}][\text{Cl}]/[\text{PF}_6]$ /water, (C) $[\text{C}_4\text{mim}][\text{BF}_4]/[\text{PF}_6]$ /water mixtures.

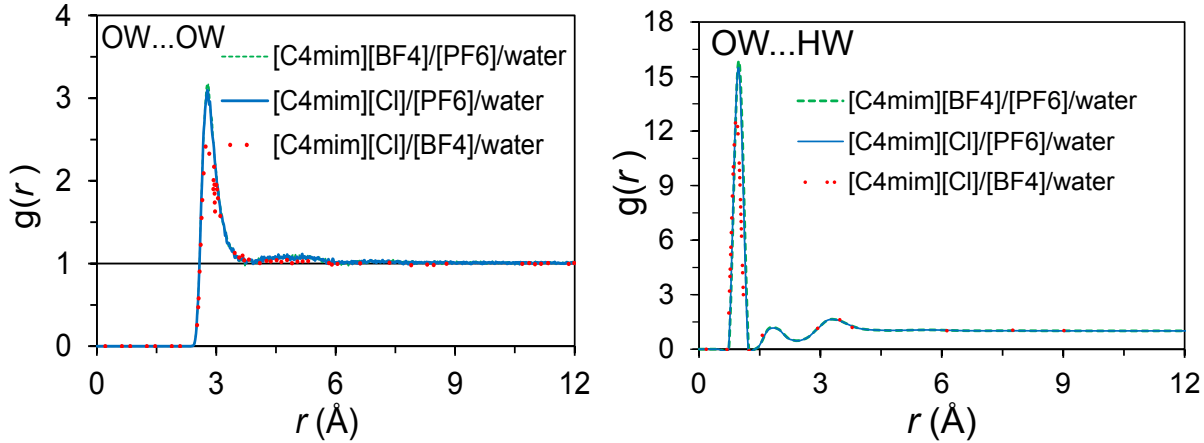


Figure S3. Radial distribution functions for the HW...OW and OW...OW interactions in aqueous mixtures.

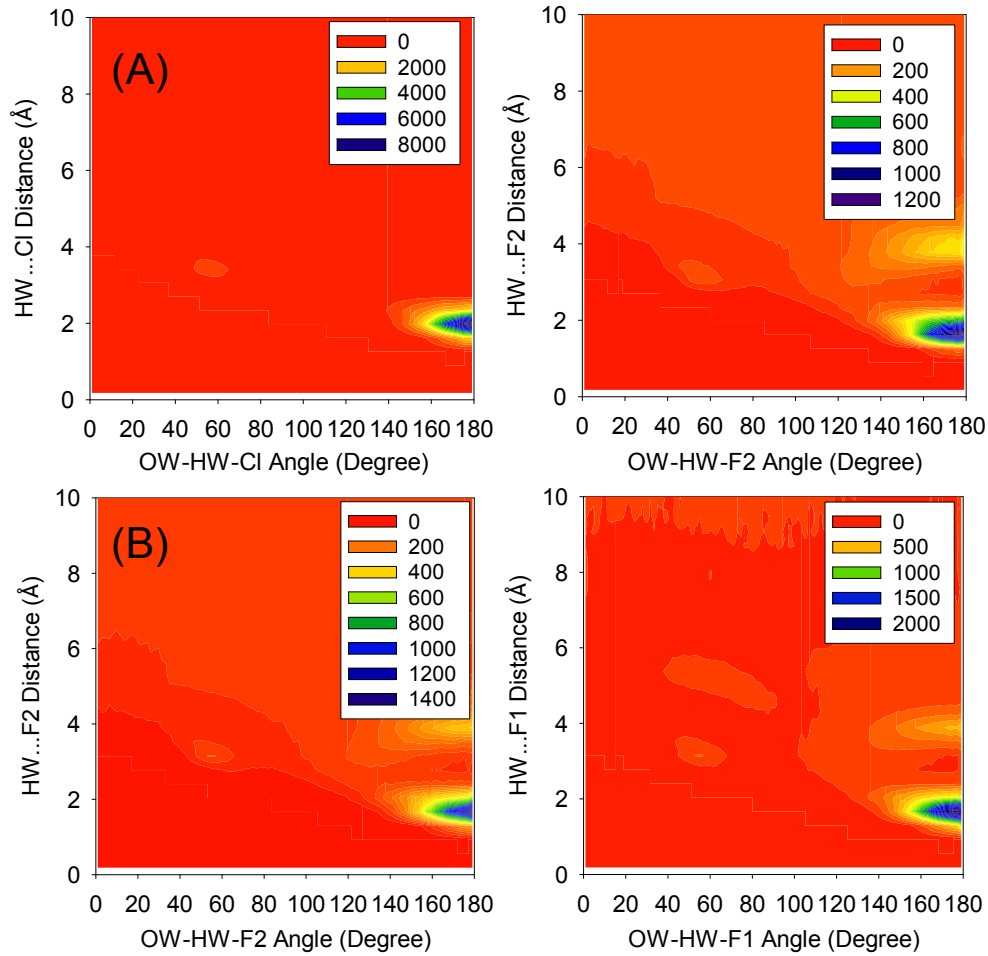


Figure S4. Combined radial/angular distribution functions of anion...water interactions for (A) [C4mim][Cl]/[PF₆]/water, and (B) [C4mim][BF₄]/[PF₆]/water systems. The RDFs were calculated between HW and the F or Cl atoms, while the angle is taken between OW, HW, and the F or Cl atoms of the anions.

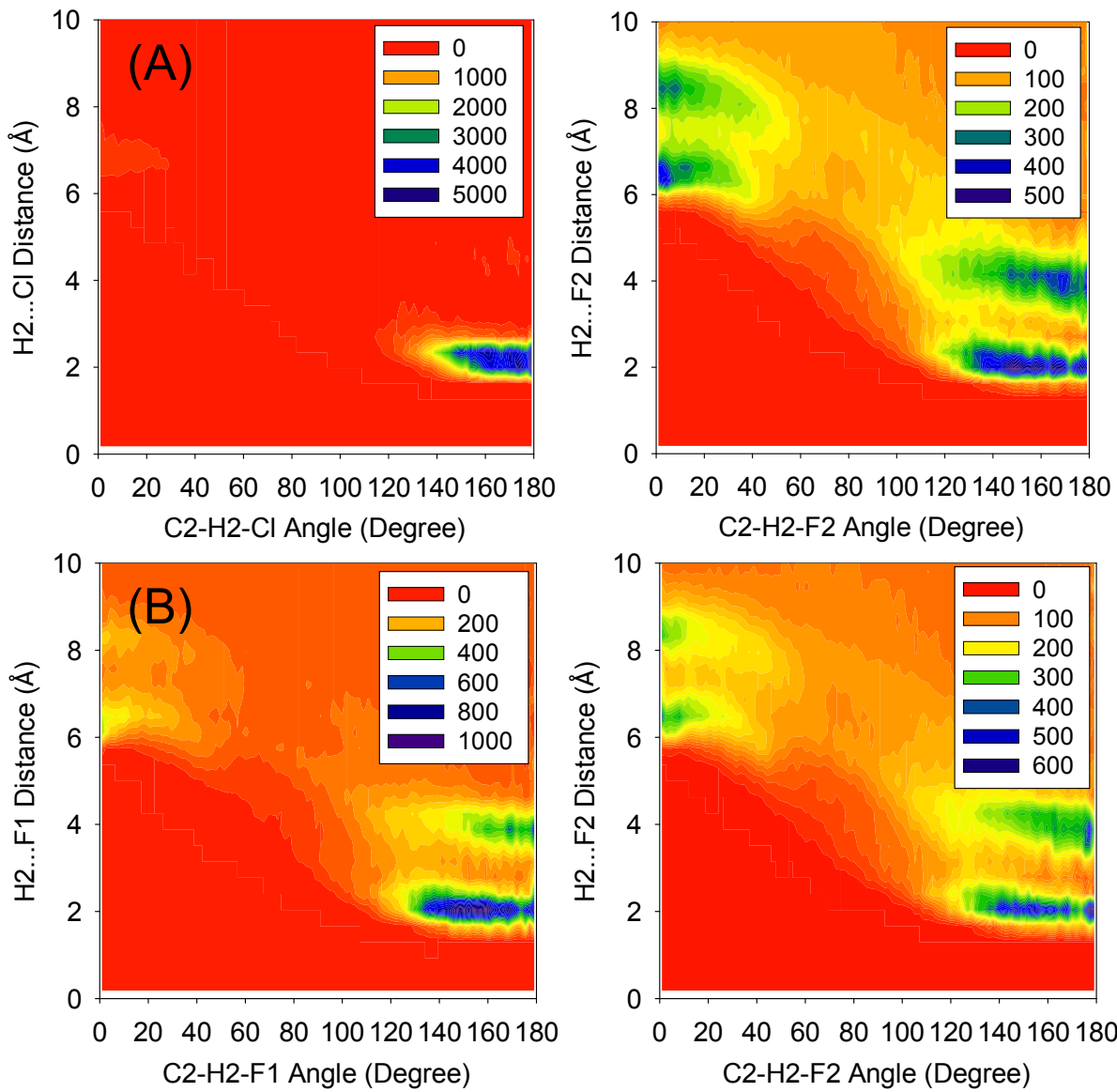


Figure S5. Combined radial/angular distribution functions of cation-anion interactions for (A) [C₄mim][Cl]/[PF₆]/water, and (B) [C₄mim][BF₄]/[PF₆]/water systems. The RDFs were calculated between H₂ and the F or Cl atoms, while the angle is taken between C₂, H₂, and the F or Cl atoms of the anions.

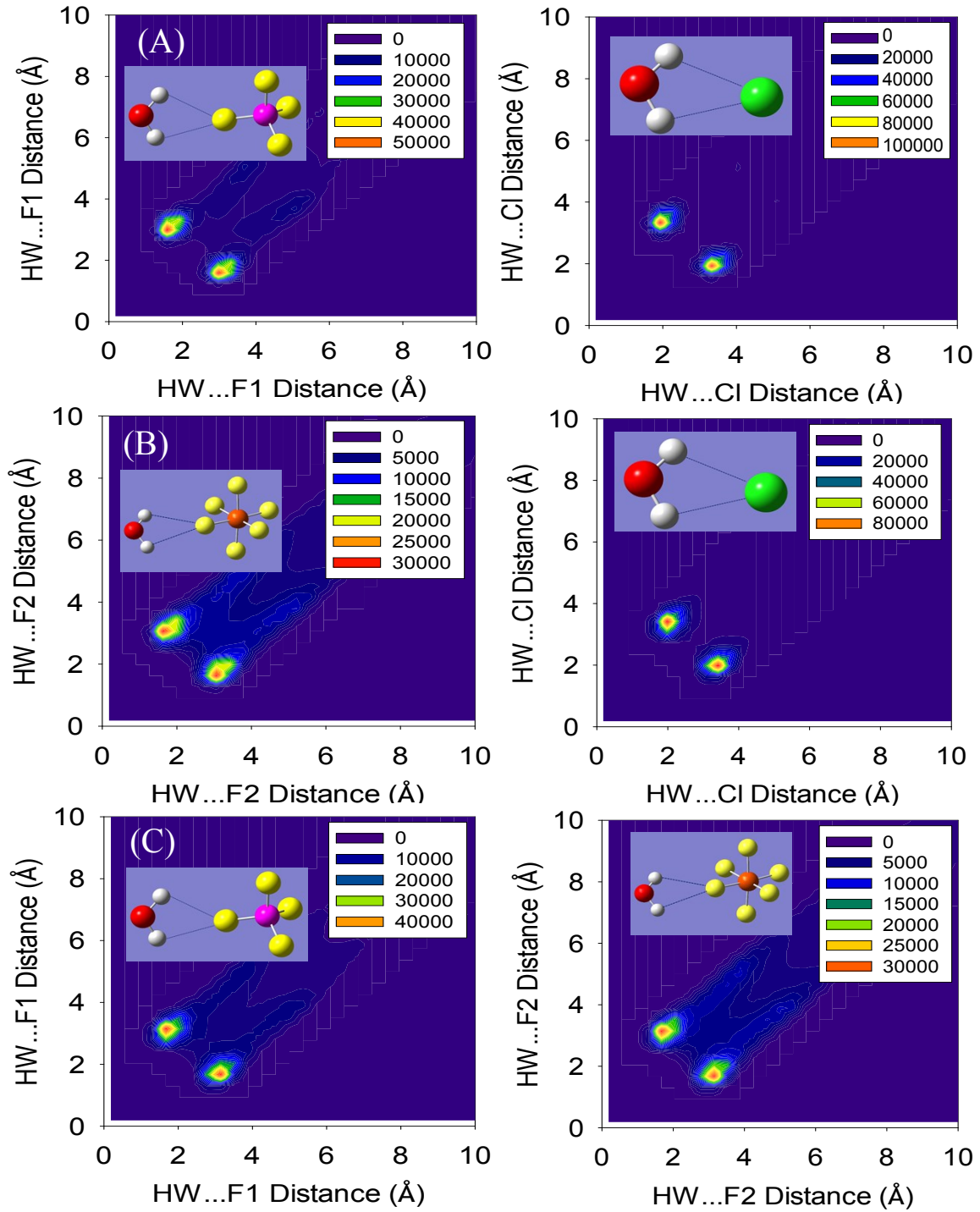


Figure S6. Combined radial/radial distribution functions for water-anion interactions of (A) [C₄mim][Cl]/[BF₄]-water, (B) [C₄mim][Cl]/[PF₆]-water, and (C) [C₄mim][BF₄]/[PF₆]-water systems.

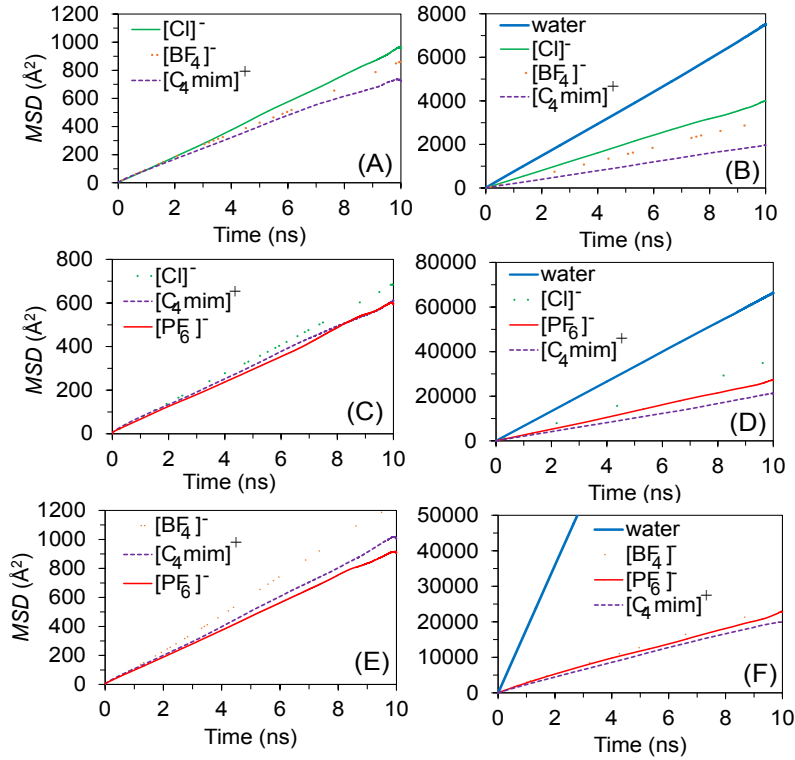


Figure S7. Mean-square displacements (MSDs) over 10 ns of simulation of the (A, B) [C₄mim][Cl]/[BF₄], (C, D) [C₄mim][Cl]/[PF₆], and (E, F) [C₄mim][BF₄]/[PF₆] systems. Left panel (A, C, and E) for the water-free systems and right panel the aqueous systems (B, D, and F).

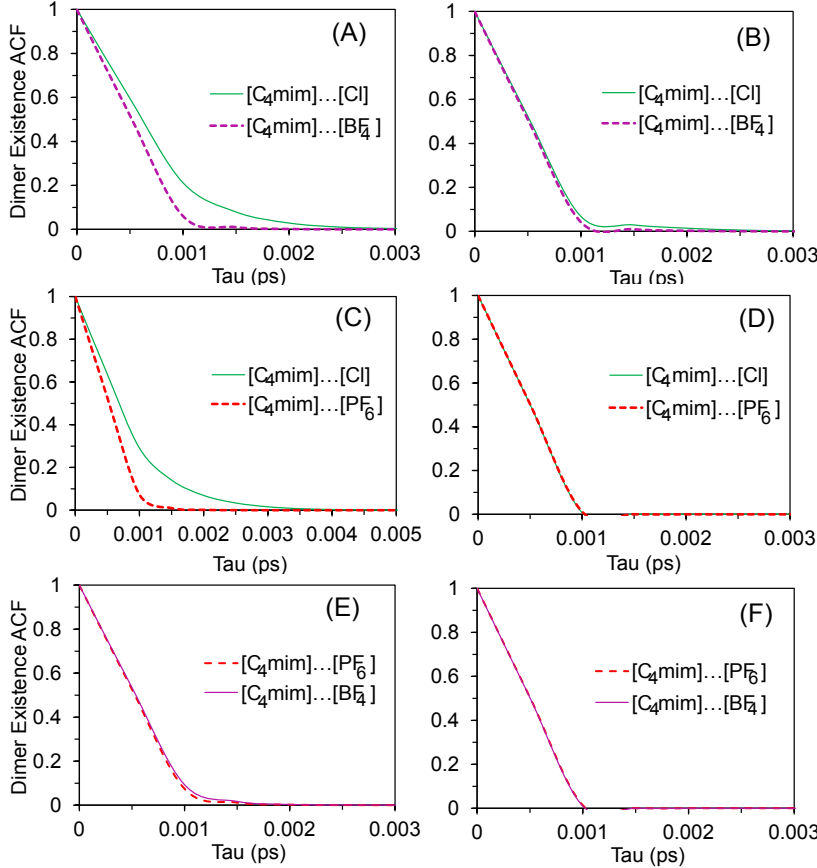


Figure S8. Dimer Existence Autocorrelation Functions (Dacf) for the (A, B) $[C_4\text{mim}][\text{Cl}]/[\text{BF}_4^-]$, (C, D) $[C_4\text{mim}][\text{Cl}]/[\text{PF}_6^-]$, and (E, F) $[C_4\text{mim}][\text{BF}_4^-]/[\text{PF}_6^-]$ systems without (left panel, A, C, and E) and with water (right panel, B, D, and F). The ion pairs are defined based on the distance criteria between Cl or F of the anions and the acidic hydrogen atom of the cations H2.

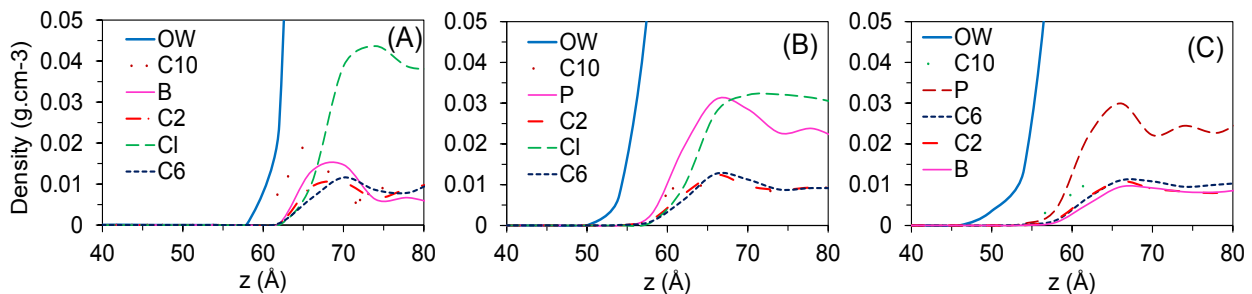


Figure S9. Atom density profiles of (A) $[C_4\text{mim}][\text{Cl}]/[\text{BF}_4^-]$ /water/vacuum, (B) $[C_4\text{mim}][\text{Cl}]/[\text{PF}_6^-]$ /water/vacuum and (C) $[C_4\text{mim}][\text{BF}_4^-]/[\text{PF}_6^-]$ /water/vacuum systems.

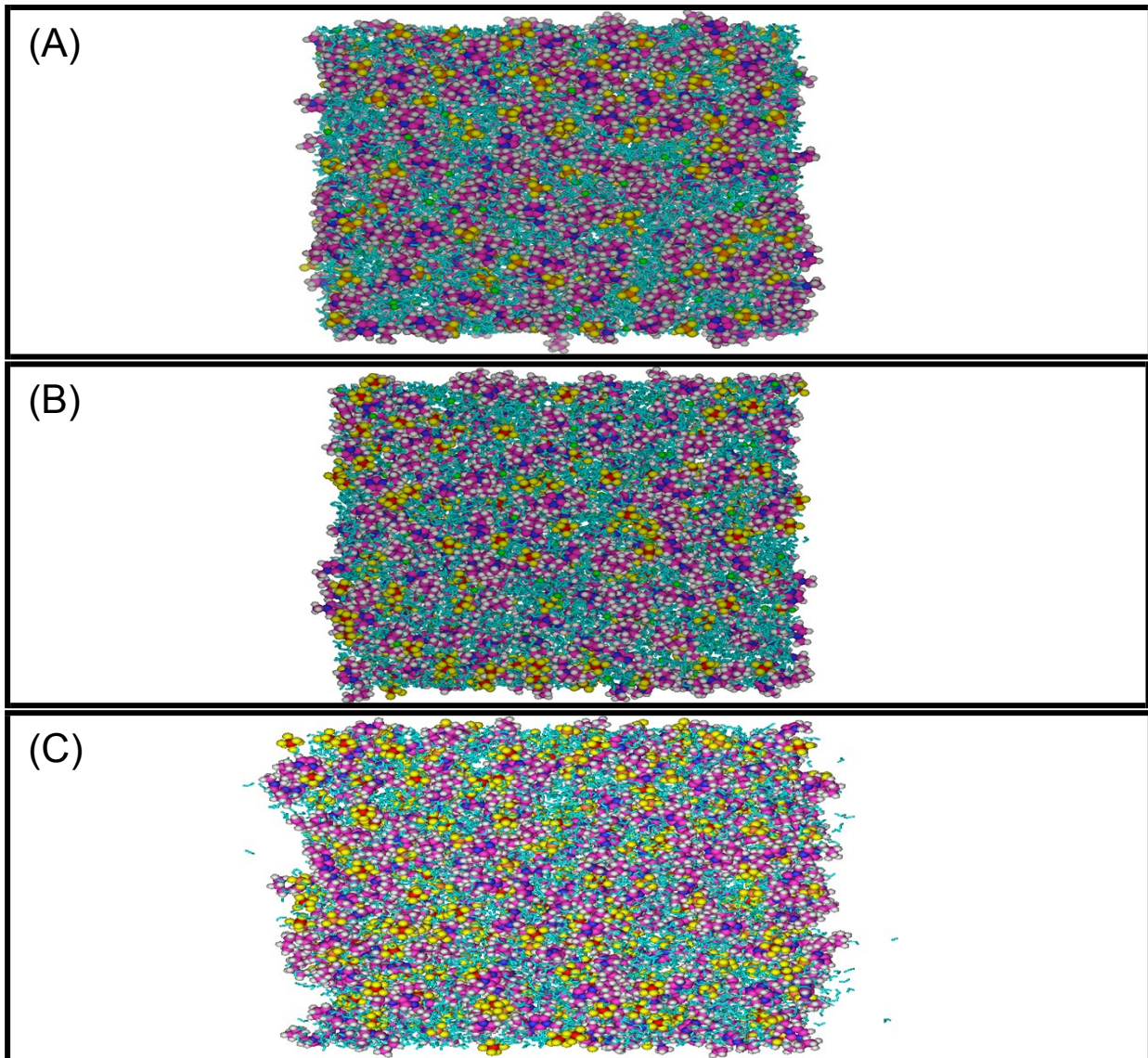


Figure S10. Snapshot after 10 ns of the simulation on the systems (A) $[\text{C}_4\text{mim}][\text{Cl}]/[\text{BF}_4]$ /water/vacuum, (B) $[\text{C}_4\text{mim}][\text{Cl}]/[\text{PF}_6]$ /water/vacuum and (C) $[\text{C}_4\text{mim}][\text{BF}_4]/[\text{PF}_6]$ /water/vacuum systems. Water molecules are plotted in light blue sticks, the IL atoms are represented as red (P), orange (B), green (Cl), yellow (F), cyan (C), white (H) and dark blue (N) spheres.

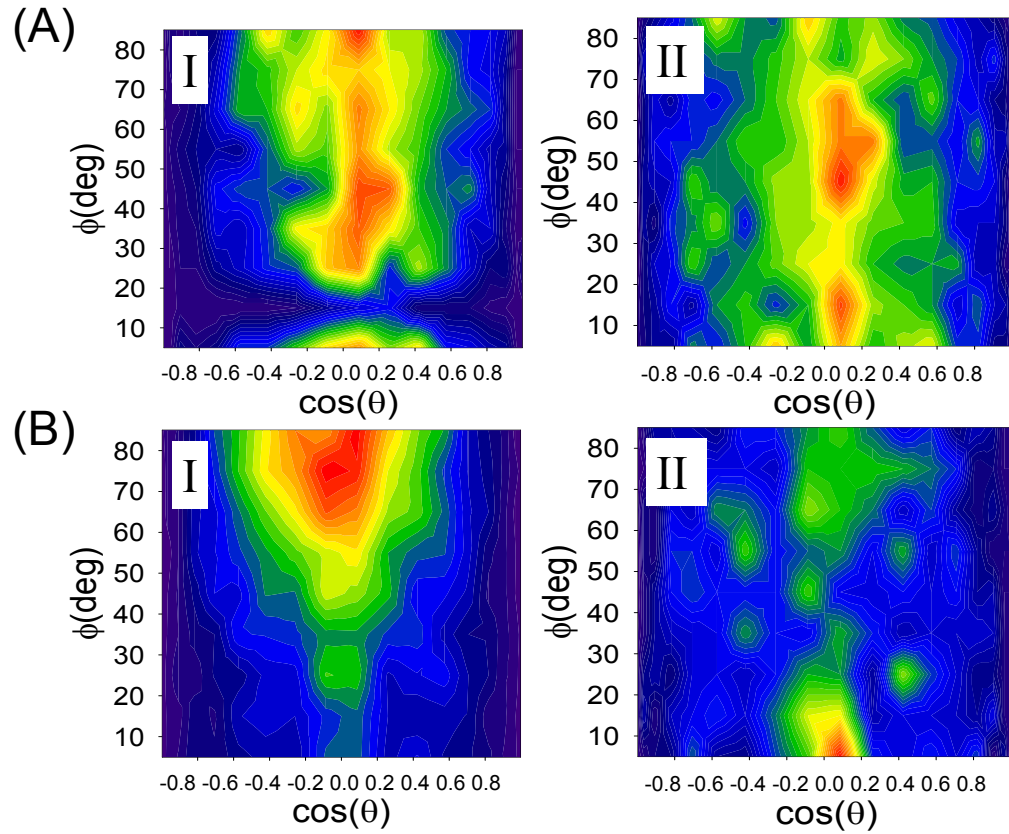


Figure S11. Bivariate orientation distribution of the $[C_4\text{mim}]^+$ cation paired to the anions for the (A) $[C_4\text{mim}][\text{Cl}]/[\text{BF}_4]$ /water/vacuum and (B) $[C_4\text{mim}][\text{Cl}]/[\text{PF}_6]$ /water/vacuum systems. Region I corresponds to a layer of 25 Å thickness and includes to the liquid/vacuum interface; region II is 25 Å thick and located in the bulk. Red corresponds to high normalized probability and dark blue corresponds to low probability.

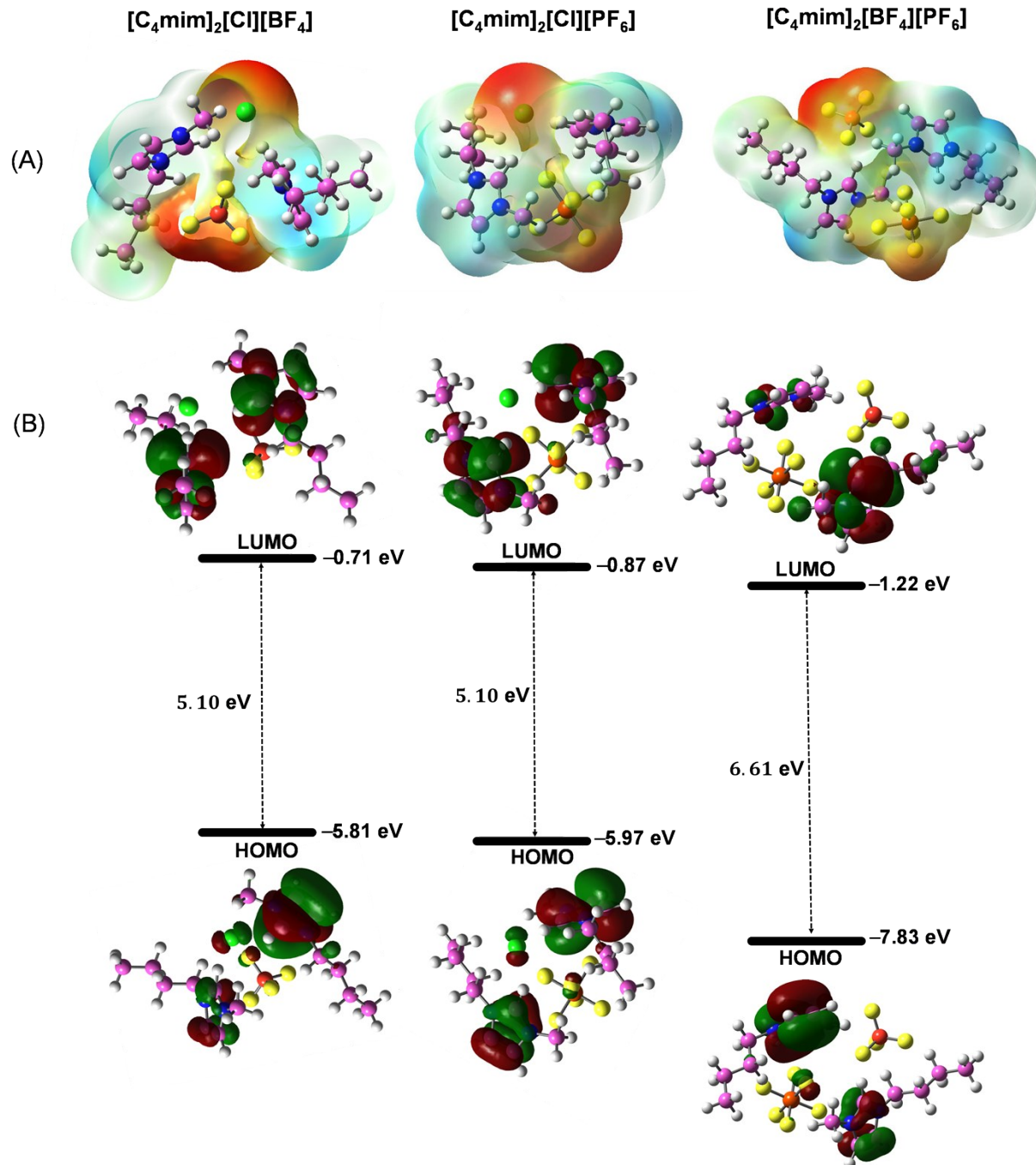


Figure S12. (A) Molecular electrostatic potential maps for binary IL complexes. MEP contours are color-coded from red (negative) to blue (positive). (B) DFT-calculated compositions of highest occupied molecular orbitals (HOMO) and lowest unoccupied molecular orbitals (LUMO) and their energies. Calculated in the gas phase at B3LYP level with 6-31+G(d,p) for all atoms, iso-surface level at 0.02 au.

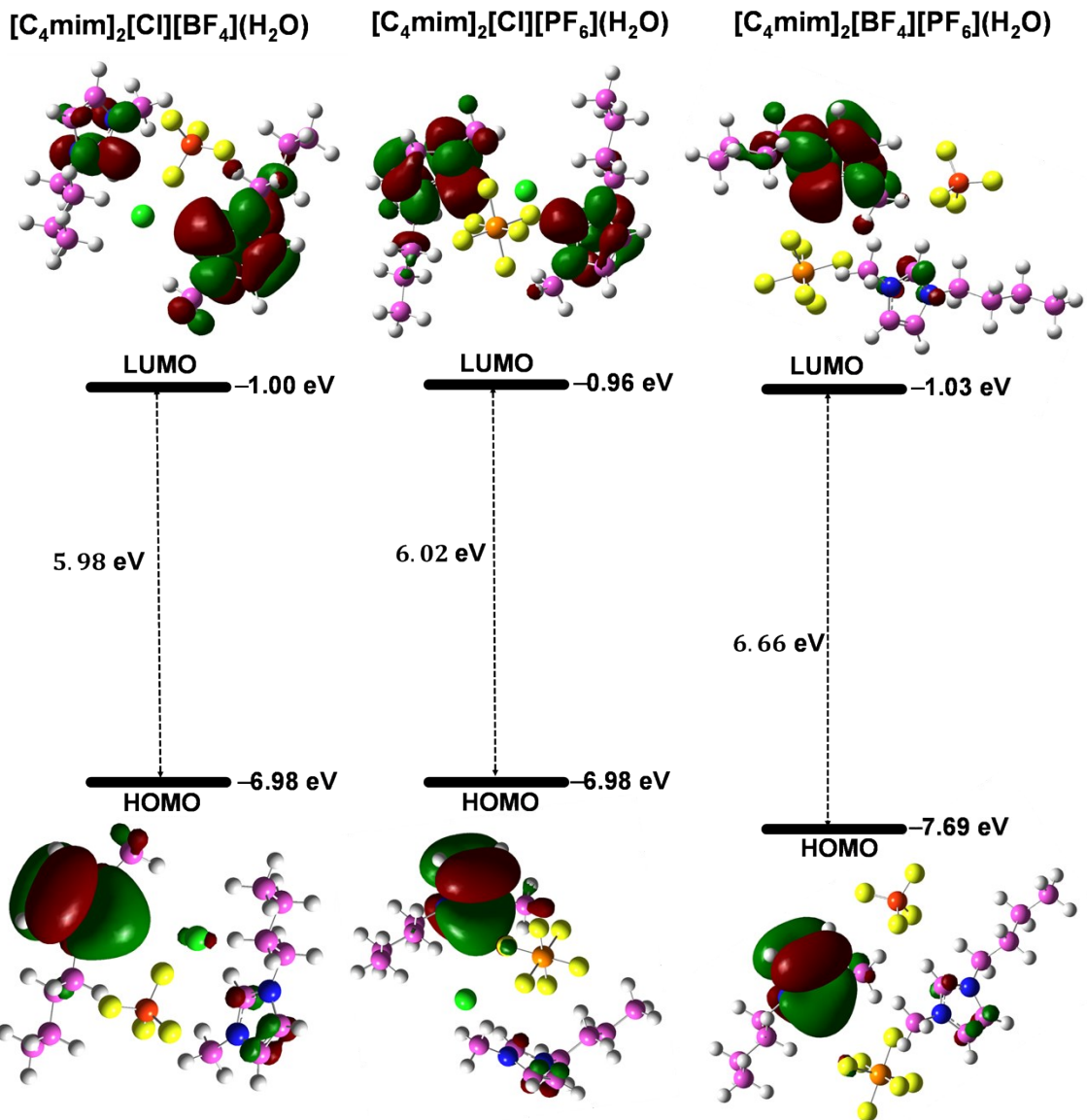


Figure S13. DFT-calculated compositions of highest occupied molecular orbitals (HOMO) and lowest unoccupied molecular orbitals (LUMO) and their energies. Calculated in the aqueous media at B3LYP level with 6-31+G(d,p) for all atoms, iso-surface level at 0.02 au.

Supporting Equations and Discussions:

$$MSD = \frac{1}{N} \left\langle \sum_{i=1}^N |r_i^c(t) - r_i^c(0)|^2 \right\rangle = \Delta|r(t)|^2 \quad (\text{Eq. S1})$$

$$D = \frac{1}{6} \lim_{t \rightarrow \infty} \frac{d}{dt} \langle [r_i^c(t) - r_i^c(0)]^2 \rangle \quad (\text{Eq. S2})$$

Dimer lifetimes of ion pairing of ILs:

In order to evaluate the lifetimes of ion pairing of ILs, the dimer existence autocorrelation function, $DACF(\tau)$, have been calculated by Travis,⁶² and for a given pair of particles i and j is defined as

$$DACF(\tau) = N \left\langle \sum_{t=0}^{T-\tau} \beta_{ij}(t+\tau) \cdot \beta_{ij}(t) \right\rangle_{ij} \quad (\text{Eq. S3})$$

$DACF(\tau)$, describes the probability that a particular ion pair is observed at a time τ , starting from the value 1 at time zero.

The lifetime of the $[\text{C}_4\text{mim}][\text{Cl}]$ ion pair was found to be longer than that of the $[\text{C}_4\text{mim}][\text{BF}_4]$ and $[\text{C}_4\text{mim}][\text{PF}_6]$ pairs in the water-free systems (Figure S8A and C). When adding water, the lifetimes of the $[\text{C}_4\text{mim}][\text{Cl}]$ ion pairs are markedly shortened and levelled to those of the $[\text{C}_4\text{mim}][\text{BF}_4]$ and $[\text{C}_4\text{mim}][\text{PF}_6]$ pairs (Figure S8B and D). For the water-free $[\text{C}_4\text{mim}][\text{BF}_4]/[\text{PF}_6]$ system the lifetimes of the $[\text{C}_4\text{mim}][\text{BF}_4]$ and $[\text{C}_4\text{mim}][\text{PF}_6]$ ion pairs are quite the same and this does not change, when water is added. This is in line with a higher ionic contribution to the binding energy of the $[\text{C}_4\text{mim}][\text{Cl}]$ ion pairs, contrasting with a higher dispersive contribution to the $[\text{C}_4\text{mim}][\text{BF}_4]$ and $[\text{C}_4\text{mim}][\text{PF}_6]$ pairs. While the former is destroyed and compensated by the $[\text{Cl}]\text{-water}$ interaction, the latter is rather independent of the presence of water. Interestingly, the strongest hydrogen donor site constitutes the H2 position at the $[\text{C}_4\text{mim}]^+$ in a water-free system, and this role is taken by the HW from H_2O in the water-containing system. This is the reason why the order of cation-Cl group's lifetime decreased. While the cation-Cl clusters possess a longer lifetime than the cation- PF_6^- aggregates in the water-free system, this trend is shown to be the same by the addition of water.